Available online at www.sciencedirect.com
SCIENCE DIRECT®
Journal of Molecular Catalysis A: Chemical 217 (2004) 175–184
JOURNAL OF MOLECULAR CATALYSIS A: CHEMICAL
www.elsevier.com/locate/molcata

Surface reactivity of NiO/Co_3O_4 and Fe_2O_3/Co_3O_4 nanocomposite catalysts: interaction with methanol

Marta Maria Natile, Antonella Glisenti*

Dipartimento di Scienze Chimiche, Università di Padova, via Marzolo, 1, 35131 Padova, Italy

Received 14 January 2004; received in revised form 14 January 2004; accepted 24 March 2004

Abstract

In this paper the reactivity of two nanocomposite supported oxides (NiO/Co_3O_4 and Fe_2O_3/Co_3O_4) toward methanol, was studied at atmospheric pressure and under high vacuum conditions.

Methanol interacts dissociatively with the Fe_2O_3/Co_3O_4 surface whereas only a weak interaction was revealed on NiO/Co_3O_4.

It is remarkable the formation, at RT, of formic acid on the surface of the NiO/Co_3O_4 supported oxide. Around 323 K the formation of carbon dioxide is evident. Formic acid is very slightly bonded to the surface and can be easily removed by a N_2 flow. In the Fe_2O_3/Co_3O_4 supported oxide is evident, besides formic acid, the formation at RT of formate species whose intensity increases with temperature.

Methanol interacts molecularly and dissociatively with both the supported oxide under HV conditions. The desorption of molecularly chemisorbed methanol is accompanied by the decomposition and fragmentation of the alcohol; at higher temperature, in contrast, oxidation and recombination reactions compete with the methoxy groups desorption.

The reactivity toward methanol of the pure and nanocomposite oxides was compared.

Keywords: Methanol oxidation; Chemisorption; Nanocomposite oxides; FTIR; Adsorption; Oxide-based catalysts; Nickel oxide; Iron oxide; Cobalt oxide; Surface reactivity

1. Introduction

Co-containing mixed oxides are already widely used in several commercial applications, such as the automotive exhausts treatment [1] or energy conversion [2]. Moreover, cobalt-based catalysts are under investigation for several interesting applications such as $DeNO_x$ catalysts [3], alcohol oxidation [4,5] or Fischer–Tropsch synthesis [6–8].

Only few studies focus on cobalt-based mixed oxides materials prepared by depositing an active oxide on a supporting one and so the unique properties of these composite systems are far from being completely understood. Moreover, oxide-based nanocomposite materials can be very interesting catalysts in oxidation reactions.

In this paper, we focus our attention on the interaction between methanol and the surface of two mixed oxides obtained depositing small particles of nickel oxide or iron oxide on Co_3O_4. Cobalt oxides are frequently supported on silica, alumina or silica–alumina. Our goal is, in contrast, to investigate the reactivity of a nanocomposite system obtained depositing an active oxide on a support that is an active catalyst. For this reason we have considered an oxides active in oxidation reactions: Co_3O_4. Cobalt oxides are used as oxidation catalysts in different reactions and, particularly, in complete oxidation reactions [1,9–11]. NiO is another component of oxidation catalysts [12] and is an interesting material for fuel cells [13,14], whereas iron oxides have been widely used in several industrial processes such as dehydrogenation, oxidation and Fischer–Tropsch synthesis [15–17]. In particular, our interest is devoted to the oxidation of methanol. Methanol is an important probe molecule being an intermediate in several oxidation reactions; moreover, it is a simple organic molecule characterised by a significant acidity. It is noteworthy that methanol can also be a promising fuel for fuel cells [18].

The two mixed oxides were obtained depositing NiO and Fe_2O_3 on Co_3O_4 and choosing a submonolayer concentration (Ni/Co and Fe/Co nominal atomic ratios = 0.05): this

* Corresponding author. Tel.: +39-049-8275196; fax: +39-049-8275161.
E-mail address: antonella.glisenti@unipd.it (A. Glisenti).

1381-1169/$ – see front matter © 2004 Elsevier B.V. All rights reserved.
doi:10.1016/j.molcata.2004.03.039

allows taking advantage of both the particular reactivity of these oxides and the nano-dimensions of the supported NiO and Fe_2O_3. Nano-scaled materials exhibit very interesting properties in catalytic applications (higher yields, as an example) attributed to the higher surface area and to the polyhedral morphology of the nanocrystals [19]. In a precedent paper [20] the nanocomposite oxides were deeply investigated. In particular a different growing mechanism was observed for the two nanocomposites; moreover, the acidic/basic sites analysis revealed significant differences with respect to the pure oxides. In this paper, we studied the interaction between the nanocomposites and methanol; the reactivity of the pure oxide powders was already investigated [21–23].

Methanol is chemisorbed both at atmospheric pressure (in nitrogen flow) and under high vacuum (HV) conditions; as a matter of fact, this should allow studying surfaces that differ with respect to their active sites. The adsorption experiment carried out at atmospheric pressure is studied by means of the diffuse reflectance infrared Fourier transform (DRIFT) spectroscopy, whereas under HV conditions X-ray photoelectron spectroscopy (XPS) and quadrupolar mass spectroscopy (QMS) have been preferred. The nanocomposite oxides show a higher oxidation capability with respect to the pure oxides and a lower bent to tie reaction intermediates or products.

2. Experimental section

The nanocomposite oxides (NiO/Co_3O_4 and Fe_2O_3/Co_3O_4) were obtained by wet impregnation of dry Co_3O_4 powder, as described in detail elsewhere [20]. The Co_3O_4 was prepared by precipitation from a basic solution of $Co(NO_3)_2{\cdot}6H_2O$ (Sigma Aldrich, 98%) [22] and calcined at 573 K. The NiO/Co_3O_4 nanocomposite oxide was prepared by wet impregnation of the cobalt oxide powder with an aqueous solution containing $Ni(NO_3)_2{\cdot}6H_2O$ (Janssen Chimica, 99%). The solid obtained after water evaporation was dried at 573 K for 10 h and calcined in air for 30 h at 973 K.

In a similar way, the Fe_2O_3/Co_3O_4 nanocomposite oxide was prepared by wet impregnation of the cobalt oxide powder with an aqueous solution containing $Fe(NO_3)_3{\cdot}9H_2O$ (Janssen Chimica, 99%). The solid obtained after water evaporation was dried at 573 K for 10 h and calcined in air for 10 h at 773 K.

Before to investigate the reactivity with respect to methanol, a careful investigation of the prepared samples was carried out by means of XPS and DRIFT spectroscopy, X-ray diffraction (XRD), thermal analysis, atomic force microscopy (AFM) and transmission electron microscopy (TEM) [20]. Moreover, the acidic and basic sites distributed on the nanocomposite oxide surfaces were studied by means of their interaction with test molecules (pyridine and carbon dioxide). The TEM images indicate that the growing mode on cobalt oxide is different for iron and nickel oxide. Iron oxide wets the surface, and small particles (ca. 5 nm) are homogeneously distributed on the support. In contrast, bigger islands of NiO (35–45 nm) grow on the cobalt oxide surface. Thermal analysis, XP and DRIFT spectroscopic techniques indicate a significant decrease of the hydroxyl groups as a consequence of the deposition of iron and nickel oxide on cobalt oxide. This result suggests the interaction of supported and supporting oxides by means of a condensation mechanism. The grafting of the supporting and supported oxide by hydroxyl condensation can determine the formation of Co–O–M (M: Fe or Ni) sites.

In order to get information on the reaction mechanism, diffuse reflectance FTIR spectra are taken with a Bruker IFS 66 spectrometer, accumulating 128 scans at a resolution of 4 cm^{-1}. The spectra are displayed in Kubelka-Munk units [25,26]. The exposure of powder samples to methanol in the IR equipment was done in an HTHP (high temperature high pressure) chamber (Spectra Tech) fitted in the Spectra-Tech. Inc. COLLECTOR^{TM} apparatus for diffuse reflectance infrared Fourier transform spectroscopy. The HTHP chamber was filled with the alcohol vapours flowing nitrogen through a bubbler containing the liquid. Methanol used for the chemisorptions was taken from a commercial source (Sigma-Aldrich, >99.9%) and used without further purification.

Prior to each experiment, 5 mg of the catalyst placed in the diffuse reflectance HTHP cell fitted with ZnSe windows were kept in nitrogen flow to eliminate water traces until a stable IR spectrum was obtained (ca. 2 h). Then, the catalyst was exposed to the alcohol for 2 min. at a flow rate of 100 ml min^{-1}, before measurement. The background spectrum of the sample before the adsorption was measured for spectra correction.

The sample temperature was measured through a thermocouple inserted into the sample holder directly in contact with the powder.

The sample for HV experiments was processed as a pellet (the powder was pressed at ca. 2×10^8 Pa for 10 min) and evacuated at 1×10^{-3} Pa for 12 h. The exposures of the pellets to methanol under HV conditions were carried out at temperatures ranging from room temperature (RT) to 673 K at a total pressure of ca. $(4–5) \times 10^{-4}$ Pa. Alcohol vapours were obtained by evaporation under vacuum. The HV reactor is directly connected to the XPS analysis chamber. The temperature of the pellet was evaluated by means of a thermocouple directly in contact with the sample holder. The surface adsorbed species were investigated by means of XPS measurements. The modification of surface nanocomposite oxide structure and composition induced by the adsorption can also be controlled by XPS. XPS spectra were recorded using a Perkin-Elmer PHI 5600 ci spectrometer with standard Al Kα and Mg Kα source (1486.6 and 1253.6 eV, respectively) working at 350 W. The working pressure was less than 1×10^{-8} Pa. The spectrometer was calibrated by assuming the binding energy (BE) of the Au $4f_{7/2}$ line to lie at 84.0 eV with respect to the Fermi level. Extended spectra

(survey) were collected in the range 0–1350 eV (187.85 eV pass energy, 0.4 eV step, 0.05 s per step). Detailed spectra were recorded for the following regions: C 1s, O 1s, Ni 2p and Co 2p (11.75 eV pass energy, 0.1 eV step, 0.1 s per step) for the sample NiO/Co_3O_4 and C 1s, O 1s, Fe 2p and Co 2p (23. 5 eV pass energy, 0.1 eV step, 0.1 s per step) for the sample Fe_2O_3/Co_3O_4. The standard deviation in the BE values of the XPS line is 0.10 eV. The atomic percentage, after a Shirley type background subtraction [27], was evaluated using the PHI sensitivity factors [28]. To account for charging problems, the C 1s peak was considered to be located at 285.0 eV, and the peak BE differences were evaluated.

The volatile products were characterised by means of a quadrupole gas analyser (European Spectrometry Systems, ESS). The QM spectra were obtained by subtracting from the spectrum recorded after chemisorption the one obtained just before. In the mass spectra the contribution of the alcohol was subtracted and the assignments were made in reference to the fragmentation patterns [29].[1] Moreover, all mass data were analysed using the method proposed by Ko et al. [30].

Desorption patterns were obtained from the mass spectra by plotting the intensities (partial pressures) of the different masses, as a function of temperature.

3. Results

3.1. Reaction with methanol under atmospheric pressure conditions: the NiO/Co_3O_4 supported oxide

DRIFT spectra obtained after exposing the NiO/Co_3O_4 supported oxide to methanol at temperatures from RT to 523 K are shown in Figs. 1 and 2 whereas in Table 1 the IR data concerning liquid- and gas-phase methanol, as well as methoxy species, are summarised.

In all the DRIFT spectra the presence of gas-phase methanol is suggested by the characteristic *P*, *Q*, and *R* rotational branches in the C–O stretching region (1013, 1032 and 1054 cm^{-1}) and is confirmed by the C–H stretching contributions [31,32]. The peaks of gaseous methanol decrease with increasing temperature.

The C–H stretching region (Fig. 1) shows a complex shape; in accordance with Busca et al. [33], the peaks at 2920, 2951, 2966 and 2980 cm^{-1} might be due to molecularly chemisorbed methanol interacting with non-equivalent surface active sites.

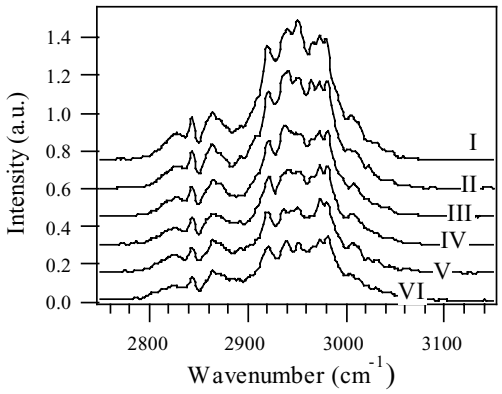

Fig. 1. DRIFT spectra obtained after exposure of the NiO/Co_3O_4 powder to methanol at different temperatures: (I) RT, (II) 323 K, (III) 373 K, (IV) 423 K, (V) 473 K, (VI) 523 K. C–H stretching region.

The N_2 flow is sufficient to remove gas-phase and molecularly chemisorbed methanol from the powder surface. In fact, no signals were observed after evacuation in the C–O and C–H stretching regions, confirming the rather low strength of the Lewis acidic sites.

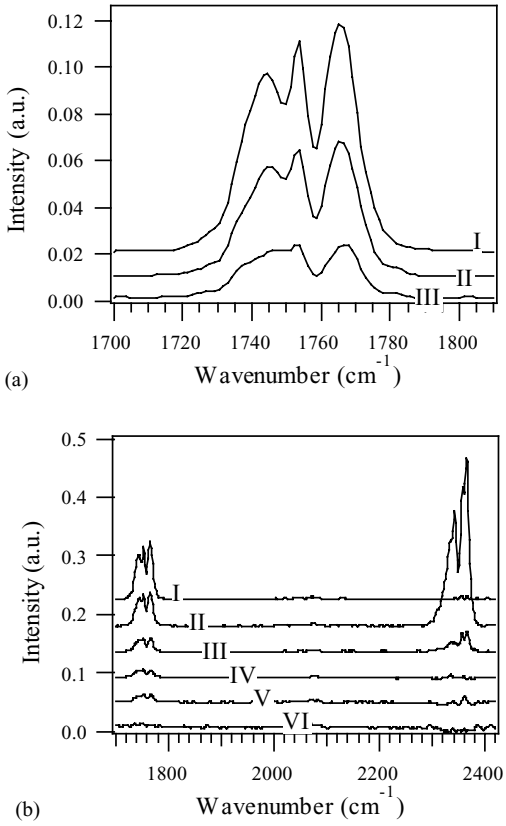

Fig. 2. DRIFT spectra obtained after exposure of the NiO/Co_3O_4 powder to methanol at different temperatures: (I) RT, (II) 323 K, (III) 373 K, (IV) 423 K, (V) 473 K, (VI) 523 K. (a) C=O stretching region, (b) region between 1700 and 2420 cm^{-1}.

[1] The contributions at 18, 31, 30 and 60 *m/e* were attributed to water, methanol, formaldehyde, and methyl-ethyl ether, respectively. The peaks at *m/e* 45 and 46 (remaining after subtracting the contribution of methyl-ethyl ether) were assigned to dimethyl-ether rather than formic acid because of the coincident signal at *m/e* 15 (expected for dimethyl-ether but not for formic acid). The peak at *m/e* 29 remaining after subtraction of the contributions of methyl-ethyl ether, dimethyl-ether and formaldehyde was attributed to the fragmentation/recombination reactions of methanol. The peak at *m/e* 28 remaining after subtraction of the contributions of methanol, formaldehyde, methyl-ethyl ether and dimethyl-ether was attributed to CO (incidentally the presence of air contamination was never observed in the HV chamber).

Table 1
IR data (cm^{-1}) of gas and liquid methanol. The IR data observed after exposure of NiO, Co_3O_4 and Fe_2O_3 to methanol are also reported

Assignments	Gas CH_3OH[a,b]	Liquid CH_3OH[a]	CH_3OH/NiO[c]	CH_3OH/Co_3O_4[d]	CH_3OH/Fe_2O_3[e]
C–O stretching	1012, 1034 vs, 1060	1029	1060–1070	1061	1070
O–H bending	1340, 1346 m	1420 m br			
CH_3 bending (a) a′′	1430 w	1420			
CH_3 bending (s) a′	1455 m	1455 m			
CH_3 bending (a) a′	1477 m	1480 sh			
CH_3 stretching (s)	2826, 2845 s (2844), 2869	2822 s	2821		2822
CH_3 stretching (a)	2973 vs (2977)	2934 vs	2921		2927
OH stretching	3673, 3687 s (3682), 3713	3337 vs br			

The IR data observed after exposure of NiO, Co_3O_4 and Fe_2O_3 to methanol are also reported.
[a] Ref. [31].
[b] Ref. [32].
[c] Ref. [21].
[d] Ref. [22].
[e] Ref. [23].

It is noteworthy that methanol dissociation is evident at $T \geq 373$ K on Co_3O_4 and at $T \geq 423$ K on NiO whereas it is never observed on the NiO/Co_3O_4 nanocomposite. The rather insignificant interaction between methanol and the NiO/Co_3O_4 surface agrees with the low presence of acidic/basic sites observed in the nanocomposite mixed oxide [20].

A remarkable result is the formation, at RT, of formic acid. This is suggested by the presence, on the DRIFT spectra, of three peaks at 1745, 1754 and 1766 cm^{-1} attributed to the C=O stretching vibration (Table 2 and Fig. 2a). Other signals at 1208, 1220 and 2940 cm^{-1} are due to formic acid. A comparison with literature data [31,34] suggests the possible formation of both monomeric and dimeric formic acid.

Inspection of the spectra obtained after exposure of the NiO/Co_3O_4 powder sample to methanol at increasing temperatures (Fig. 2a and b) reveals that the peaks attributed to formic acid decrease with increasing temperature and new signals around 2342 and 2364 cm^{-1} appear at 323 K. These new peaks are attributed to the formation of carbon dioxide suggesting that formic acid is decomposed; at about 473 K both formic acid and carbon dioxide disappear.

The DRIFT spectra obtained after exposing the supported oxide powder to methanol and successively to N_2 at different temperatures, are shown in Fig. 3; inspection of the spectra shows that formic acid is slightly bonded to the surface and can be removed by N_2. CO_2 more strongly interacts with the NiO/Co_3O_4 surface and is not completely removed by N_2 at 323 K.

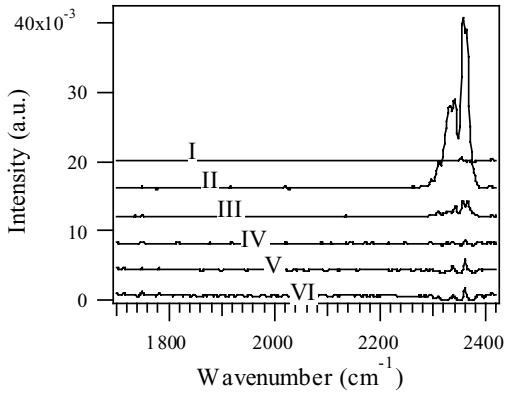

Fig. 3. DRIFT spectra obtained after exposure of the NiO/Co_3O_4 powder to methanol and successively to N_2 at different temperatures: (I) RT, (II) 323 K, (III) 373 K, (IV) 423 K, (V) 473 K, (VI) 523 K: region between 1700 and 2460 cm^{-1}.

3.2. Reaction with methanol under atmospheric pressure conditions: the Fe_2O_3/Co_3O_4 supported oxide

DRIFT spectra obtained after exposing the Fe_2O_3/Co_3O_4 supported oxide to methanol from RT to 473 K are shown in Figs. 4–6.

Table 2
IR data (cm^{-1}) of monomer and dimeric formic acid

Assignments	HCOOH monomer[a,b]	$(HCOOH)_2$[b]	$HCOOH/Fe_2O_3$[c]	NiO/Co_3O_4[d]	Fe_2O_3/Co_3O_4[d]
C–O stretching	1093, 1206 vs	1030 sh, 1218 vs	1216	1208, 1220	1208, 1220
C=O stretching	1740 vs, 1770 vs	1754 vs	1735–1745	1745, 1754, 1766	1746, 1754, 1765
C–H stretching	2940 s, 2943	2957 vs	2939	2940, 2951	2947

The data obtained after exposure of Fe_2O_3 to formic acid are also reported as well as the values obtained in the present work upon exposing the nanocomposite oxides to methanol.
[a] Ref. [32].
[b] Ref. [34].
[c] Ref. [35].
[d] This work.

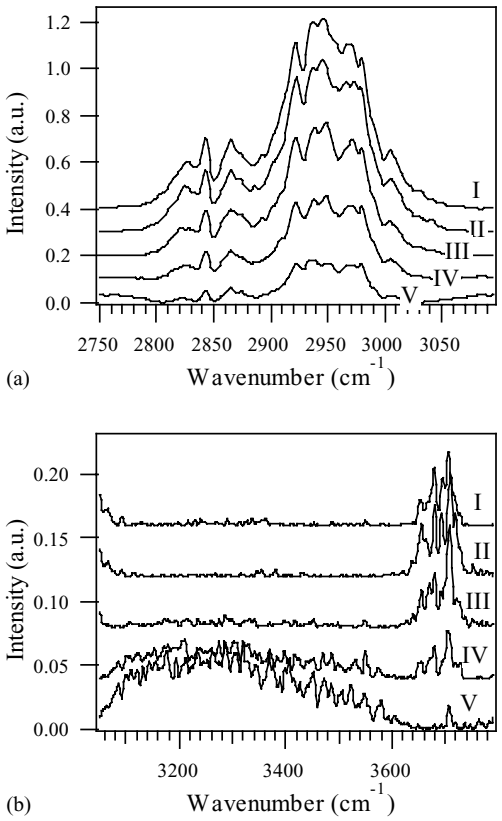

Fig. 4. DRIFT spectra obtained after exposure of the Fe_2O_3/Co_3O_4 powder to methanol at different temperatures: (I) RT, (II) 323 K, (III) 373 K, (IV) 423 K, (V) 473 K. (a) C–H stretching region, (b) O–H stretching region.

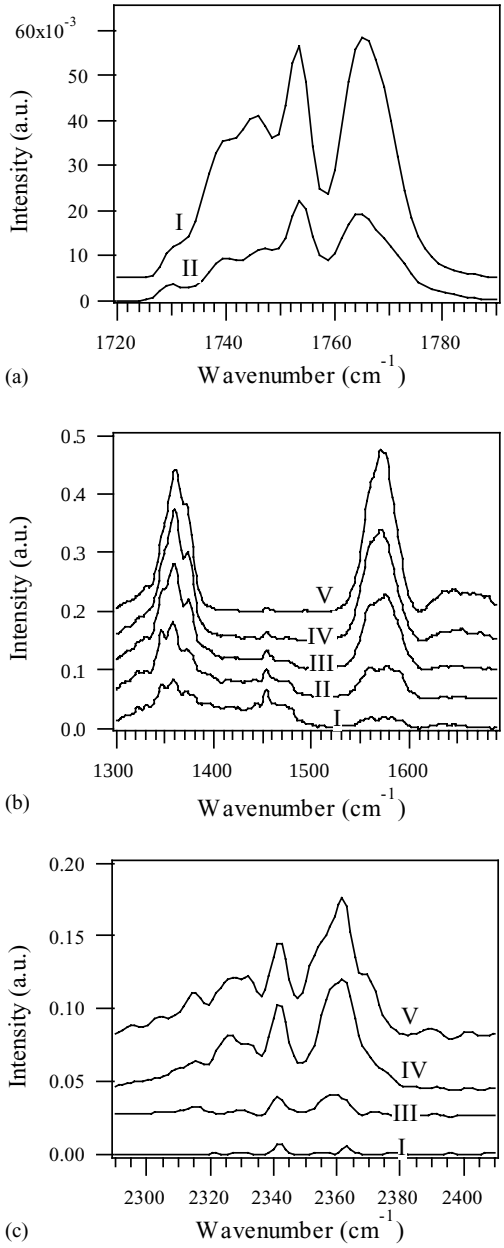

Fig. 5. DRIFT spectra obtained after exposure of the Fe_2O_3/Co_3O_4 powder to methanol at different temperatures: (I) RT, (II) 323 K, (III) 373 K, (IV) 423 K, (V) 473 K. (a) C=O stretching region, (b) region between 1300 and 1690 cm^{-1}, (c) region between 2280 and 2410 cm^{-1}.

The DRIFT spectrum obtained at RT shows, in addition to the gas-phase methanol, the formation of methoxy groups, as suggested by the shoulder around 1060 cm^{-1} (C–O stretching) and by the peaks at 2822 and 2921 cm^{-1} (symmetric and asymmetric C–H stretching, Fig. 4a) [23]. The peaks attributed to the methoxy species can be easily observed in the spectra obtained after exposing to methanol and successively to N_2 (Fig. 6a). Several peaks centred at about 1020, 1027–1040, 1057 and 1068–1075 cm^{-1} suggest the presence of methoxy species interacting with non-equivalent surface active sites [18,21] and/or with a different adsorption geometry. Consistently, in the O–H stretching region (Fig. 4b) several contributions at about 3600–3750 cm^{-1} arise upon exposure to methanol at RT. The OH signal at higher wavenumbers shows several contributions: 3652, 3668 (shoulder), 3680, 3696, 3707, 3717 (shoulder) and 3727 cm^{-1}; some signals (3652, 3668 and 3717 cm^{-1}) correspond to those observed after exposure of the α-Fe_2O_3 to methanol at RT [23]. The intensity of these signals decreases with the temperature increment; after exposure to methanol at 473 K, only the peaks at 3707 and 3717 cm^{-1}, corresponding to isolated OH groups, are evident on the oxide surface [23,35].

A broad band at 3000–3600 cm^{-1} becomes evident at higher temperatures (423 K) and agrees with the presence of molecularly chemisorbed water (3400–3600 cm^{-1}). The formation of water on the oxide surface is also confirmed by the corresponding O–H bending peak at 1640 cm^{-1} and suggests a condensation mechanism between methanol and the surface hydroxyl groups.

DRIFT results indicate methanol dissociation at RT and agree with the formation of new acidic sites observed when nanoparticles of Fe_2O_3 are deposited on Co_3O_4 [20]. Methanol dissociation occurs through two different mechanisms: direct dissociation is prevalent at low temperature, whereas dissociation by interaction with the hydroxyl groups is prevalent at high temperature [21,22].

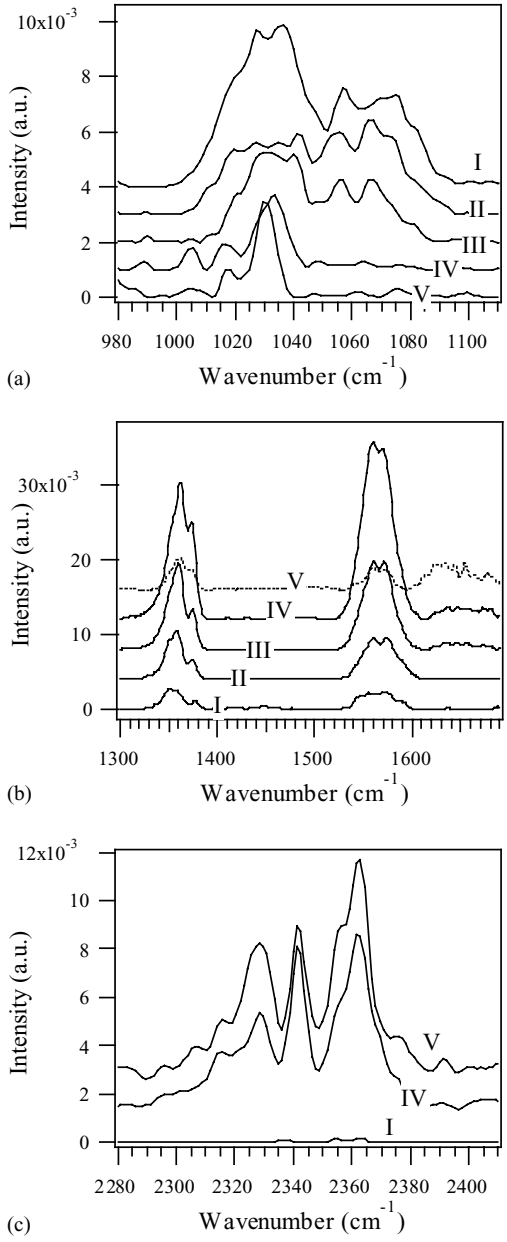

Fig. 6. DRIFT spectra obtained after exposure of the Fe_2O_3/Co_3O_4 powder to methanol and successively to N_2 at different temperatures: (I) RT, (II) 323 K, (III) 373 K, (IV) 423 K, (V) 473 K. (a) C–O stretching region, (b) region between 1300 and 1690 cm^{-1}, (c) region between 2280 and 2410 cm^{-1}.

The peaks of gas-phase methanol and the signals attributed to methoxy groups decrease with the temperature increment.

At RT, the formation of formic acid is evident as on NiO/Co_3O_4 surface. This result is suggested by the presence of three peaks at 1745, 1754 and 1765 cm^{-1} (C=O stretching vibration—Table 2 and Fig. 5a) and by the peaks at 1208, 1220 cm^{-1} (C–O stretching) and 2947 cm^{-1} (C–H stretching) [34,35]. The signals at 1220, 1745, and 2947 cm^{-1} correspond to those observed upon exposing α-Fe_2O_3 to HCOOH [35].

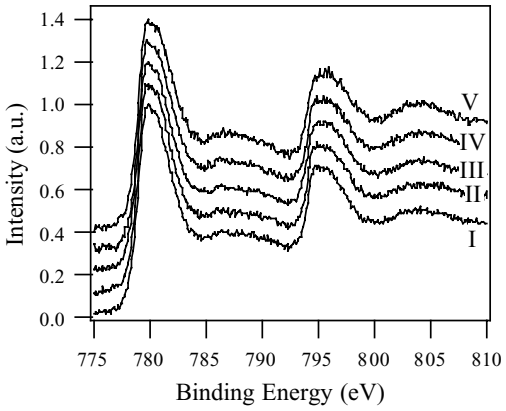

Fig. 7. Co 2p XP spectra of NiO/Co_3O_4 obtained (I) before and after the exposure to methanol at (II) RT, (III) 423 K, (IV) 573 K, (V) 673 K (the spectra are normalised with respect to their maximum value).

Unlike the NiO/Co_3O_4 supported oxide, the formation of formate species is evident at RT, as suggested by the peaks at 1340–1380, 1571 cm^{-1} (Fig. 5b) and by the shoulder at 2867 cm^{-1} (symmetric C–H stretching—Fig. 4a) [36]. Noteworthy, only formate forms ($T > 400$ K) when α-Fe_2O_3 is exposed to methanol. The position of the observed peaks agrees with the results obtained after exposing the α-Fe_2O_3 to methanol (1358, 1379 and 1583 cm^{-1}) and are slightly higher than those observed after adsorption of formic acid (1371 and 1558 cm^{-1}) [35]. The different position of the IR signals, suggests different adsorption geometry of the formate species obtained through different pathways: as a matter of fact, the oxidation of methanol to formate should proceed through the inclusion of lattice oxygen [21].

In the Fe_2O_3/Co_3O_4 sample formate species increase with temperature. Two new peaks at 2341 and 2362 cm^{-1} are present in the spectrum recorded after exposure at 373 K; these peaks, due to CO_2, increase with temperature and are still evident at 473 K (Fig. 5c). The conversion to CO_2 was only observed at $T > 470$ K when formate originates from the dissociation of formic acid on the α-Fe_2O_3 surface whereas the presence of CO_2 was never observed in the IR spectra obtained after exposing hematite to methanol at increasing temperature. These results suggest a different reactivity for formate species derived by different pathways.

Nitrogen completely removes formic acid whereas traces of carbon dioxide, formate, and water are always present on the Fe_2O_3/Co_3O_4 supported oxide surface (Fig. 6b and c).

3.3. Reaction with methanol under HV conditions: the NiO/Co_3O_4 supported oxide

The Co 2p and O 1s XP spectra observed before and after exposure to methanol are shown in Figs. 7 and 8. The Co $2p_{3/2}$ peak position (780.1 eV) and shape (Fig. 7) agree with the expected values for Co_3O_4 (780.3 eV) [20,22,28,37] and do not change after exposure to the alcohol at RT. The chemisorption at higher temperatures, in contrast, partially

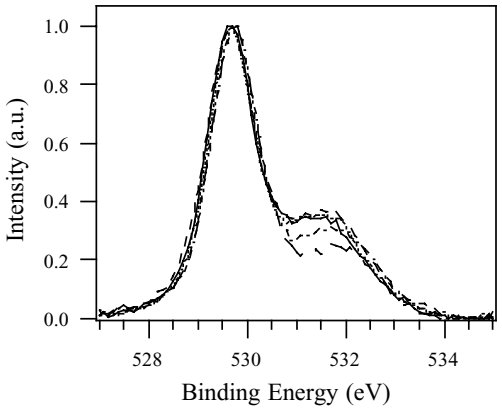

Fig. 8. O 1s XP spectra of NiO/Co_3O_4 obtained (—) before and after the exposure to methanol at (···) RT, (- - -) 423 K, (-·-·-) 573 K, (– – –) 673 K (the spectra are normalised with respect to their maximum value).

reduces the supporting oxide surface as suggested by the intensity increment of the Co(II) shake-up peaks in the Co 2p region (at 787.0 and 804.0 eV) [38].[2] The Ni $2p_{3/2}$ peak shows several contributions characteristic of Ni(II): at about 854.0 eV (Ni–O bonds), 855.4 eV (Ni–OH bonds and multiplet splitting of the Ni–O peak) and 861.4 eV (shake-up signal) [20,21,28,37]. The position and shape of the Ni 2p peak are not modified by the chemisorptions at high temperatures. The O 1s peak position (529.6 eV) is due to the M–O bonds (M: Ni or Co), whereas a tail toward the high binding energy side is indicative of M–OH bonds [20–22,28,37]. The oxygen signal (Fig. 8) does not change significantly upon exposure to methanol at RT. A slight increment of the high BE tail suggests the formation of new hydroxyl groups on the supported oxide surface at 423 K. At higher temperature the tail at higher binding energy (ca. at 531.5 eV), attributed to M–OH bonds, decreases progressively as a consequence of the heat treatments under HV. The experimental Ni/Co atomic ratio (=0.10) remains unchanged, whereas the O/(Ni + Co) atomic ratio decreases from 1.55 (upon exposure at RT) to 1.39 (upon exposure at 773 K) confirming the reduction of the mixed oxide surface.

The QMS data (Fig. 9) show the desorption of molecularly chemisorbed methanol at temperatures lower than ca. 373–423 K whereas methoxy groups desorb at higher temperatures (ca. 473 K). CO, H_2O, CO_2 and H_2, as well as fragmentation products, desorb with the molecularly chemisorbed methanol. At higher temperatures oxidation products prevail. Around 623 K, a signal with $m/e = 30$ suggests the desorption of formaldehyde; the formation of formaldehyde from methanol competes with the decomposition of the alcohol to water and carbon oxides but in this HV experiment the lower presence of oxygen probably facilitates the formation of intermediate products instead of formic acid.

[2] The XP spectra of Co(II) high-spin compounds, such as CoO, are characterised by an intense shake-up satellite structure at ca. 787.0 and 804.0 eV. Unlike in Co(II) compounds, in the low-spin Co(III) compounds, the satellite structure is weak or missing. Co_3O_4, a mixed-valence oxide, shows a weak satellite structure symptomatic of shake-up from the minor Co(II) component.

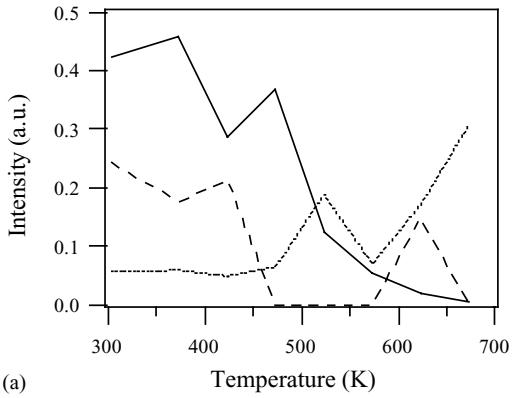

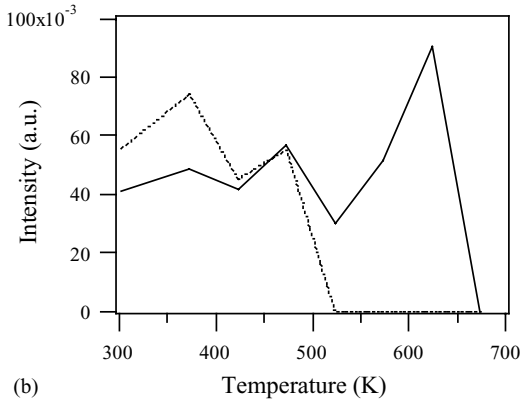

Fig. 9. Desorption patterns obtained after exposure of the NiO/Co_3O_4 powder to methanol. (a) (—) CH_3OCH_3, (- - -) CH_3CH_2, (···) and $H_2O/4$; (b) (—) CO_2, (···) $CH_3CH_2OCH_3$.

3.4. Reaction with methanol under HV conditions: the Fe_2O_3/Co_3O_4 supported oxide

The XPS spectra obtained after exposing the Fe_2O_3/Co_3O_4 supported oxide to methanol at different temperatures, are shown in Figs. 10 and 11. The Fe $2p_{3/2}$ peak position (711.3 eV) agrees with literature data for Fe_2O_3 as confirmed by the Fe(III) shake-up peak at 718.9 eV (Fig. 10) [20,23,28,37–40]. The Fe 2p peak does not change upon exposure to methanol at RT, whereas in the Co 2p region the increment of the shake-up peaks (at ca. 787.0 and 804.0 eV) is evident and suggests the surface reduction of the Co_3O_4 support (as observed for NiO/Co_3O_4) to CoO. This result confirms that the formation of formate from methanol proceeds through the inclusion of lattice oxygen, as already hypothesised when discussing the DRIFT data.

The O 1s peak shows three components at 530.1, 531.4 and 533.1 eV; the two contributions at lower BE are attributed to the M–O and M–OH bonds (M: Fe or Co), respectively, whereas the component at 533.1 eV agrees with the presence of different M–OH bonds or chemisorbed

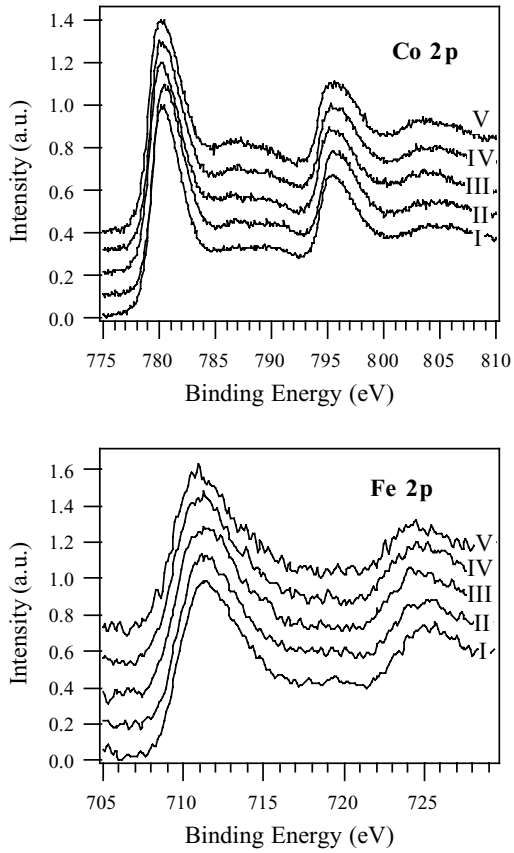

Fig. 10. Fe 2p and Co 2p XP spectra of Fe_2O_3/Co_3O_4 obtained (I) before and after the exposure to the methanol at (II) RT, (III) 423 K, (IV) 523, (V) 673 K (the spectra are normalised with respect to their maximum value).

water [20,22,23,28,37–40]. The high BE tail of the O 1s peak attributed to the hydroxyl groups, increases after the exposure to methanol at RT as a consequence of the alcohol dissociation. The component at 531.4 eV decreases upon exposure at higher temperatures (as a consequence of the hydroxyl groups condensation), whereas the contribution at 533.0 eV remains almost unchanged. The Fe/Co atomic ratio (=0.10) is not modified by the exposure to methanol at RT or at higher temperatures. The O/(Fe + Co) atomic ratio decreases, from 1.44, before the chemisorptions, to 1.30, after the chemisorption at 673 K confirming the reduction of Co_3O_4.

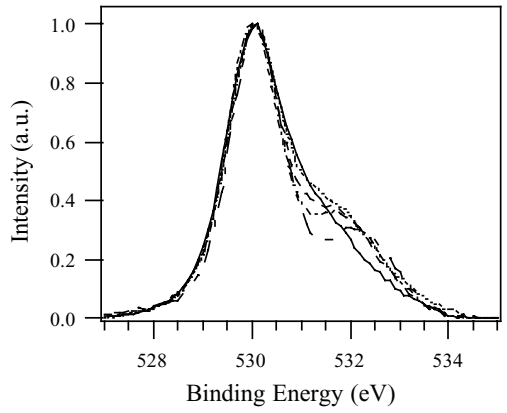

Fig. 11. O 1s XP spectra of Fe_2O_3/Co_3O_4 obtained (—) before and after the exposure to methanol at (···) RT, (---) 423 K, (-·-·-) 523 K, (–––) 673 K (the spectra are normalised with respect to their maximum value).

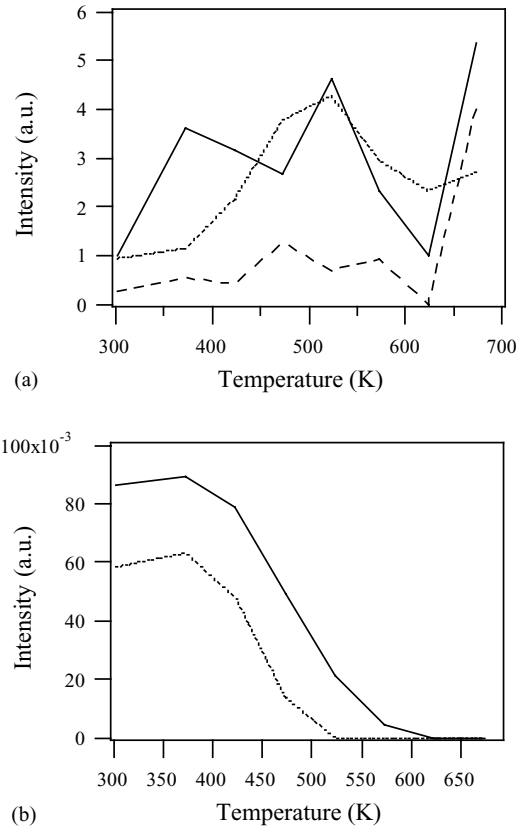

Fig. 12. Desorption patterns obtained after exposure of the Fe_2O_3/Co_3O_4 powder to methanol. (a) (—) CH_3OH, (···) CO, (---) $CO_2 \times 10$; (b) (—) $CH_3OCH_3/3$, (···) $CH_3CH_2OCH_3$.

Molecularly chemisorbed methanol desorbs (Fig. 12) at low temperatures and the QM spectra only show the desorption of methoxy species around 373 and 523 K. The peak at 373 K is accompanied by the desorption of fragmentation reaction products (mainly dimethyl ether and methyl-ethyl ether). At higher temperature (523 K) the methoxy species desorbs, in contrast, with the concomitant formation of water and carbon oxides (mainly CO). Similarly to the NiO/Co_3O_4 supported oxide, is evident at 623 K the presence in the QM spectra of formaldehyde.

4. Discussion

Several mechanisms of interaction between alcohol molecules and oxide surfaces are possible depending on the degree of surface hydroxylation [21–23] and on the strength of the Lewis and Brønsted acidic and basic surface sites. Methanol can adsorb molecularly with an oxide surface interacting with the hydroxyl groups (by means of

H-bonds) or with the Lewis acidic sites; the replacement of water molecules eventually adsorbed on the oxide surface can be another possibility. When dissociative interaction takes place, as in Fe_2O_3/Co_3O_4, the involved mechanisms can be rather different. On a dehydroxylated surface the dissociation can involve directly the Lewis acidic and basic sites to produce hydroxyl groups and alkoxy groups. Otherwise a condensation reaction between methanol and surface hydroxyl groups can give rise to methoxy species and water molecules.

In a precedent paper, we observed that the NiO/Co_3O_4 and Fe_2O_3/Co_3O_4 mixed oxide surfaces are only slightly hydroxylated [20]. This is demonstrated by the DRIFT and XP spectroscopic techniques results: the presence of hydroxyl groups is only evidenced by XPS, as summarised in the experimental session. In such a situation the interaction mechanisms involving OH groups or water molecules cannot be significant. Moreover, an increment of hydroxyl groups was observed after the exposure of the Fe_2O_3/Co_3O_4 nanocomposite oxide to methanol. For this surfaces, then, a direct dissociation mechanism with the formation of hydroxyl and alkoxy groups can be suggested; a similar mechanism was observed on the Co_3O_4 surface exposed to methanol at 373 K [22]. A condensation mechanism is only evident at 423 K.

It is noteworthy that the dissociation products are more evident on the Fe_2O_3/Co_3O_4 mixed oxide surface with respect to the Co_3O_4 surface. This result agrees with the formation of new acidic/basic sites observed in the Fe_2O_3/Co_3O_4 nanocomposite material with respect to the supporting oxide [20]. These sites, evidenced by their interaction with pyridine, are both Lewis (1621, 1630 cm^{-1}) and Brønsted (1654 cm^{-1}) acidic sites. The complex sites constituted by a Fe(III) cation and its neighbouring oxygen atom, in contrast, were observed on hematite but disappear in the mixed oxide [24]. A different behaviour is evident on the NiO/Co_3O_4 oxide, which shows less acidic/basic sites than the pure Co_3O_4: the rather weak Lewis acidic sites observed on the Co_3O_4 powder surface (whose interaction with pyridine gives rise to a pick at 1603 cm^{-1}) are not observed on the NiO/Co_3O_4 nanocomposite catalyst. For this reason the NiO/Co_3O_4 nanocomposite, shows a very low capability to interact with methanol. Noteworthy, the NiO/Co_3O_4 nanocomposite surface does not interact with the formic acid or the carbon dioxide originated by methanol oxidation and can easily release the products.

The differences observed in acidic/basic sites distribution and strength can deeply influence the redox behaviour of the samples. Formic acid is evident on both the supported oxide surfaces at RT suggesting that new active redox sites form on the surfaces of the nanocomposite oxides attributing them a higher oxidation power.

In fact, α-Fe_2O_3 gives rise to formate at $T \geq 400$ K [23], whereas its presence is evident on Fe_2O_3/Co_3O_4 exposed to methanol at RT. Similarly, formic acid forms at RT on NiO/Co_3O_4 whereas methanol gives rise to formate both on the NiO and Co_3O_4 powder samples (at $T \geq 423$ and 373 K, respectively) and to CO_2 on NiO at 373 K (in both the cases the oxidation products are tightly bonded to the surface). Moreover, the formation of water and carbon dioxide upon exposing Fe_2O_3/Co_3O_4 to methanol at increasing temperature is evident at 373 K, whereas the formation of carbon dioxide upon exposure of α-Fe_2O_3 to methanol was only evident at temperatures higher than 470–500 K.

Significant considerations can be drawn by the comparison of the QMS results obtained in HV; under vacuum conditions hydrocarbons form as a consequence of the adsorption of methanol on Fe_2O_3, whereas water and carbon dioxide are generated only when a mixture of methanol and oxygen is used [23]. The results obtained when methanol is adsorbed on the Fe_2O_3/Co_3O_4 nanocomposite oxide are, in contrast, similar to those observed on the Co_3O_4 powder: the formation of dimethyl and methyl-ethyl ethers is evident at $T < 500$–600 K whereas CO forms at $T > 400$–450 K.

In the NiO/Co_3O_4 nanocomposite oxide CO_2 is revealed by QMS at $T < 600$–650 K. The formation of methyl-ethyl ether and dimethyl ether is evident at $T < 500$–600 K in the NiO/Co_3O_4 nanocomposite as well as in the NiO powder whereas the desorption of H_2O and CO_2 is evident in the NiO powder sample from 550 to 700 K and at $T < 500$ K in the Co_3O_4.

These results, as a whole, could indicate that the differences in reactivity evidenced in the mixed with respect to the pure oxides may be related to rather weak active sites that can be destroyed by the vacuum condition. Moreover, different oxygen mobility in the mixed oxides, probably related to structural properties, should be also considered.

5. Conclusions

In this paper, the interaction between methanol and two nanocomposites oxides (NiO/Co_3O_4 and Fe_2O_3/Co_3O_4) was studied and compared with the behaviour of the pure oxides.

The investigated nanocomposite oxides are characterised by the following XPS atomic ratios: Ni/Co = 0.10 (nominal atomic ratio = 0.05) and Fe/Co = 0.10 (nominal atomic ratio = 0.05). The NiO and Fe_2O_3 particles deposited on Co_3O_4 show different sizes (diameter is 5 nm for Fe_2O_3/Co_3O_4 and 35–45 nm for NiO/Co_3O_4).

The dissociation of methanol is evident on Fe_2O_3/Co_3O_4 whereas only a very weak interaction is observed with NiO/Co_3O_4.

At RT, the formic acid forms on the surface of the NiO/Co_3O_4 supported oxide. The peaks due to formic acid decrease with the temperature whereas around 323 K the formation of carbon dioxide is evident. Around 473 K both formic acid and carbon dioxide are not anymore visible. Formic acid is very slightly bonded to the surface and can be easily removed by a N_2 flow.

Formic acid also forms on the surface of the Fe_2O_3/Co_3O_4 supported oxide exposed to methanol at RT. Unlike the case of the NiO/Co_3O_4 supported oxide, in this case is evident

the formation, at RT, of formate species whose intensity increases with temperature. CO_2 forms at $T \geq 373$ K. Formic acid is removed by N_2, whereas traces of carbon dioxide and formate are always present.

The HV adsorption experiment shows, for the NiO/Co_3O_4 supported oxide, the desorption of molecularly chemisorbed methanol at temperatures lower than ca. 373 K whereas methoxy groups desorb at higher temperatures. CO, H_2O, CO_2 and H_2, as well as fragmentation products desorb with the molecularly chemisorbed methanol whereas, at higher temperatures, the oxidation reactions prevail. Around 623 K the dehydrogenation of methanol to formaldehyde competes with the decomposition of the alcohol to water and carbon oxides.

Molecularly chemisorbed methanol desorbs from the Fe_2O_3/Co_3O_4 supported oxide at temperatures lower than from NiO/Co_3O_4. The desorption patterns show the presence of fragmentation/decomposition and recombination product, similarly to the NiO/Co_3O_4 case, whereas at higher temperatures oxidation products prevail.

Acknowledgements

The authors gratefully acknowledge Professor E. Tondello for helpful discussions.

References

[1] J.J. Spivey, Ind. Eng. Chem. Res. 26 (1987) 2165.
[2] N.M. Sammes, M. Brown, I.W.M. Brown, J. Mater. Sci. 31 (1996) 6060.
[3] O. Ciambelli, P. Corbo, M.C. Gaudino, F. Migliardini, D. Sannino, Top. Catal. 16/17 (2001) 413.
[4] J. Llorca, N. Homs, J. Sales, P. Ramírez de la Piscina, J. Catal. 209 (2002) 306.
[5] T.-C. Xiao, S.-F. Ji, H.-T. Wang, K.S. Coleman, M.L.H. Green, J. Mol. Catal. A: Chem. 175 (2001) 111.
[6] P.J. Van-Berge, J. Van de Loosdrecht, S. Barradas, A.M. Van der Kraan, Catal. Today 58 (2000) 321.
[7] R. Oukaci, A.H. Singleton, J.G. Goodwin, Appl. Catal. A 186 (1999) 129.
[8] M.J. Keyser, R.C. Everson, R.L. Espinoza, Appl. Catal. A 171 (1998) 99.
[9] D.G. Castner, Ph.R. Watson, I.Y. Chan, J. Phys. Chem. 93 (1989) 3188.
[10] M. Shirai, T. Inona, H. Onishi, K. Asakura, Y. Iwasawa, J. Catal. 145 (1994) 159.
[11] G.A. Somorjai, Introduction to Surface Chemistry and Catalysis, Wiley, 1994.
[12] A. Barresi, I. Mazzarino, B. Ruggeri, Chim. Ind. 71 (1989) 64.
[13] P.C. Gravelle, S.J. Teichner, Adv. Catal. 167 (1969) 20.
[14] F. Tietz, F.J. Dias, D. Simwonis, D. Stover, J. Eur. Ceram. Soc. 20 (2000) 1023.
[15] L. Daza, C.M. Rangel, J. Baranda, M.T. Casais, M.J. Martinez, J.A. Alonso, J. Power Source 86 (2000) 329.
[16] H.H. Kung, Transition Metal Oxides: Surface Chemistry and Catalysis, Elsevier, Amsterdam, 1989.
[17] C.K. Rofer-DePoorter, Chem. Rev. 81 (1981) 447.
[18] J. Larmine, A. Dicks, Fuel Cell Systems Explained, Wiley, 2000.
[19] K.J. Klabunde, Nanoscale Materials in Chemistry, Wiley/Interscience, 2001.
[20] M.M. Natile, A. Glisenti, Chem. Mater. 15 (2003) 2502.
[21] M.M. Natile, A. Glisenti, Chem. Mater. 14 (2002) 4895.
[22] M.M. Natile, A. Glisenti, Chem. Mater. 14 (2002) 3090.
[23] A. Glisenti, G. Favero, G. Granozzi, J. Chem. Soc., Faraday Trans. 94 (1998) 173.
[24] L. Ferretto, A. Glisenti, J. Mol. Catal. A: Chem. 187 (2002) 119.
[25] P. Kubelka, F. Munk, Z. Tech. Phys. 12 (1931) 593.
[26] G. Kortum, Reflectance Spectroscopy, Springer, New York, 1969.
[27] D.A. Shirley, Phys. Rev. 55 (1972) 4709.
[28] J.F. Moulder, W.F. Stickle, P.E. Sobol, K.D. Bomben, in: J. Chastain (Ed.), Handbook of X-ray Photoelectron Spectroscopy, Physical Electronics, Eden Prairie, MN, 1992.
[29] S.G. Lias, S.E. Stein, NIST/EPA/MSDC Mass Spectral Database PC Version 3.0, June 1990.
[30] E.I. Ko, J.B. Benzinger, R.J. Madix, J. Catal. 62 (1980) 264.
[31] M. Falk, E. Whalley, J. Chem. Phys. 34 (1961) 1554.
[32] G. Herzberg, Infrared and Raman Spectra of Polyatomic Molecules, Van Nostrand, New York, 1949.
[33] G. Busca, P.F. Rossi, V. Lorenzelli, M. Benaissa, J. Travert, J.-C. Lavalley, J. Phys. Chem. 89 (1985) 5433.
[34] R.C. Millikan, K.S. Pitzer, J. Am. Chem. Soc. 80 (1958) 3515.
[35] A. Glisenti, J. Chem. Soc., Faraday Trans. 94 (1998) 3671.
[36] G. Busca, J. Lamotte, J.-C. Lavalley, V. Lorenzelli, J. Am. Chem. Soc. 109 (1987) 5197.
[37] X-ray Photoelectron Spectroscopy Database 20, Version 3.0, National Institute of Standards and Technology, Gaithersburg, MD.
[38] D. Briggs, J.C. Riviere, in: D. Briggs, M.P. Seah (Eds.), Practical Surface Analysis, Wiley, New York, 1983;
N.S. McIntyre, M.G. Cook, Anal. Chem. 47 (1975) 2208.
[39] D. Briggs, J.C. Riviere, in: D. Briggs, M.P. Seah (Eds.), Practical Surface Analysis, Wiley, New York.
[40] N.S. McIntyre, D.G. Zetaruk, Anal. Chem. 49 (1977) 1521.